Journal of
Materials Chemistry A

RSC Publishing

PAPER

View Article Online
View Journal | View Issue

Published on 21 June 2013. Downloaded by City University of Hong Kong on 06/08/2013 11:31:17.

Cite this: *J. Mater. Chem. A*, 2013, **1**, 9942

Developing controllable anisotropic wet etching to achieve silicon nanorods, nanopencils and nanocones for efficient photon trapping†

Hao Lin,‡[ad] Ho-Yuen Cheung,‡[b] Fei Xiu,‡[a] Fengyun Wang,[a] SenPo Yip,[a] Ning Han,[a] TakFu Hung,[a] Jun Zhou,[d] Johnny C. Ho*[ac] and Chun-Yuen Wong*[b]

Received 14th May 2013
Accepted 20th June 2013

DOI: 10.1039/c3ta11889d

www.rsc.org/MaterialsA

Controllable hierarchy of highly regular, single-crystalline nanorod, nanopencil and nanocone arrays with tunable geometry and etch anisotropy has been achieved over large areas (>1.5 cm × 1.5 cm) by using an [$AgNO_3$ + HF + HNO_3/H_2O_2] etching system. The etching mechanism has been elucidated to originate from the site-selective deposition of Ag nanoclusters. Different etch anisotropies and aspect ratios can be accomplished by modulating the relative concentration in the [$AgNO_3$ + HF + HNO_3/H_2O_2] etching system. Minimized optical reflectance is also demonstrated with the fabricated nano-arrays. Overall, this work highlights the technological potency of utilizing a simple wet-chemistry-only fabrication scheme, instead of reactive dry etching, to attain three-dimensional Si nanostructures with different geometrical morphologies for applications requiring large-scale, low-cost and efficient photon trapping (*e.g.* photovoltaics).

Introduction

In recent years, due to their unique optical, electrical and extraordinary surface-area-to-volume properties, three-dimensional (3-D) silicon (Si) nanostructures such as nanowires, nanopillars and nanocones have been extensively explored for solar cells, sensors, vertical transistors and so forth.[1–12] In fact, most of these structures have been fabricated with reactive ion etching (RIE) in order to achieve a high aspect ratio, in which the substantial processing cost, low throughput, fluorine contamination as well as the induced surface roughness may potentially restrict the practical implementation of these nanostructures for technological applications.[13,14] For example, plasma chemistry was utilized to form sharp Si nanocone arrays though the control of RIE etching conditions.[15,16] In contrast, the conventional wet anisotropic etching approach, producing sharp and well-controlled features, still has not been well achieved in part because the chemical etchants preferentially erode the underlying substrate equally in all directions.[17] Here, we utilize a facile wet-chemistry-only fabrication scheme for the controllable hierarchy of highly regular, single-crystalline and high aspect ratio Si nanostructures with different geometrical morphologies, ranging from nanorod, nanopencil and nanocone arrays. Importantly, these nano-arrays can be manipulated with tunable dimensions and spacing over a wide range in large areas, which is particularly attractive for applications requiring efficient photon trapping (*e.g.* photovoltaics).

Experimental details

The Si nanopillar arrays used as fabrication templates were prepared by the well-known nano-sphere lithography process followed by metal-assisted chemical etching,[18,19] and the preparation schematic is shown in the ESI Fig. S1.† Briefly, monodispersed polystyrene (PS) nanospheres were assembled into a close-packed monolayer on boron-doped p-type Si (100) substrates with a resistivity of 1–10 ohm cm using the Langmuir–Blodgett (LB) method. The substrates were pre-treated with mild oxygen plasma to induce hydrophilic surfaces for the facilitation of uniform nanosphere coating. The diameter and spacing of the spheres can be further manipulated by subsequent oxygen plasma etching. Utilizing these spheres as the mask, a 1.5/20 nm thick Ti/Au mesh film can be deposited through thermal evaporation and Si nanopillars with a controllable diameter and periodicity can be achieved *via* metal catalytic etching in HF/H_2O_2 solution.

Once the templates were obtained, they were treated with a mixture of $AgNO_3$, HF, and HNO_3 or H_2O_2. This mixture has a

[a]Department of Physics and Materials Science, City University of Hong Kong, 83 Tat Chee Ave., Kowloon Tong, Kowloon, Hong Kong. E-mail: johnnyho@cityu.edu.hk; Fax: +852-34420538; Tel: +852-34424897

[b]Department of Biology and Chemistry, City University of Hong Kong, 83 Tat Chee Ave., Kowloon Tong, Kowloon, Hong Kong. E-mail: acywong@cityu.edu.hk

[c]Centre for Functional Photonics (CFP), City University of Hong Kong, 83 Tat Chee Avenue, Kowloon Tong, Kowloon, Hong Kong

[d]Department of Physics, Ningbo University, Ningbo, People's Republic of China

† Electronic supplementary information (ESI) available: Fig. S1: processing details about the fabrication of Si nanopillars as the template; Fig. S2: SEM images of various dimensions of nanocones. See DOI: 10.1039/c3ta11889d

‡ These authors contributed equally to this work.

This journal is © The Royal Society of Chemistry 2013

Published on 21 June 2013. Downloaded by City University of Hong Kong on 06/08/2013 11:31:17.

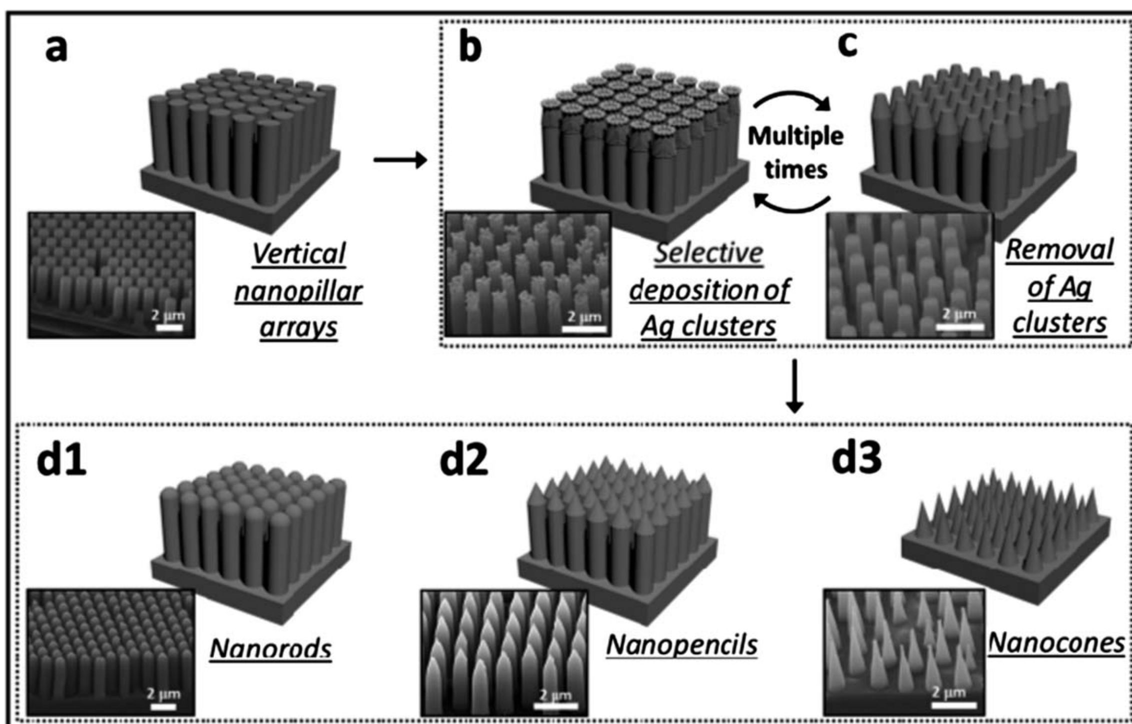

Fig. 1 Process schematics for the formation of different morphological nanopillar arrays. The insets show the representative SEM images of these nano-arrays (pitch = 1.3 μm).

dual function: it leads to the selective deposition of Ag clusters at the nanopillar tips and at the same time performs Si etching (see Results and discussion below for the etching mechanism). This way, the subsequent removal of Ag clusters by HNO_3 washing would give truncated nanopillar tips as depicted in the process schematic in Fig. 1. These Ag cluster deposition and removal processes were then repeated multiple times in order to yield different morphological nanopillar arrays tailored under well-controlled chemical conditions. The figure also illustrates representative scanning electron microscopy (SEM) images of the fabricated nanopillar, nanorod, nanopencil and nanocone arrays with a uniform height of ~2 to 3 μm and a structural pitch of 1.3 μm in these structures. Notably, the morphologies, dimensions and aspect ratios of these nano-arrays can be controlled accurately over large areas (>1.5 cm × 1.5 cm) with this simple wet-chemistry technique (Fig. 2).

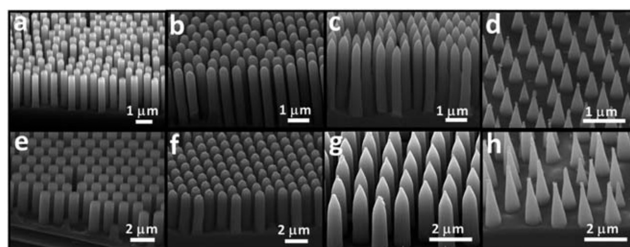

Fig. 2 SEM images of the fabricated high-aspect (a and e) nanopillar, (b and f) nanorod, (c and g) nanopencil, (d and h) and nanocone arrays for the pitch of 0.6 and 1.3 μm, respectively.

Surface morphologies of fabricated Si nano-arrays were examined with a scanning electron microscope (SEM, FEI/Philips XL30) and a transmission electron microscope (TEM, Philips CM-20). Crystal structures were determined by imaging with a high resolution TEM (JEOL 2100F) and selected area electron diffraction (SAED, Philips CM-20). Elemental mappings were performed using an energy dispersive X-ray (EDS) detector attached to the JEOL 2100F to measure the chemical composition of etched nano-arrays. For the elemental mapping and TEM, the nano-arrays were first harvested onto the grid for the corresponding characterization.

Results and discussion

Selective deposition of Ag nanoclusters

It is well known that the combination of HNO_3 and HF represents the most common isotropic etchants for Si, in which HNO_3 serves as an oxidant to convert Si to SiO_2 while HF etches the oxide.[20–24] However, the [$AgNO_3$ + HF + HNO_3/H_2O_2] system in this work leads to anisotropic etching of Si. The origin of this etch anisotropy can be attributed to the introduction of $AgNO_3$, which gives rise to the generation of Ag nanoclusters on Si nanopillars. AgF is known to react with Si to yield Ag due to the redox reaction $4AgF + Si \rightarrow 4Ag + SiF_4$.[25] With the [$AgNO_3$ + HF + HNO_3] system as the wet chemical etchant shown in Fig. 1 and 2, the interplay of (1) Ag formation aforementioned, (2) SiO_2 formation by the oxidation of HNO_3, and (3) SiO_2 etching by HF leads to the formation of Ag nanoclusters at the nanopillar tips in this work. The Ag nanoclusters were experimentally

Published on 21 June 2013. Downloaded by City University of Hong Kong on 06/08/2013 11:31:17.

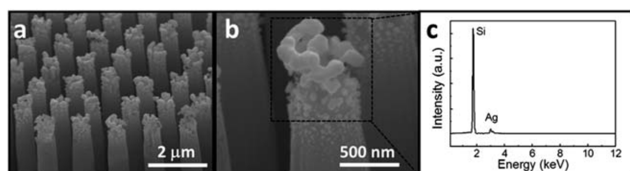

Fig. 3 (a) SEM image of the Si nanopillar arrays after the selective deposition of Ag nanoclusters. (b) Zoom-in image of the Si nanopillar tips, demonstrating the selective coating of Ag nanoclusters (only on the tips but not on the base). (c) EDS spectrum of the tip region, confirming the presence and chemical content of pure Ag nanoclusters.

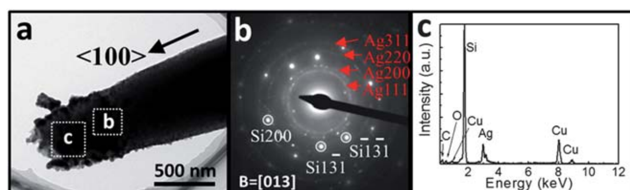

Fig. 4 (a) TEM image of the representative Si nanopillar tip after selective deposition of Ag nanoclusters. (b) SAED pattern in the location "b" of the Si nanopillar tip, illustrating the existence of polycrystalline Ag nanoclusters selectively coated onto the Si nanopillar tips. Also, the diffraction pattern indicates the Si nanopillar axial direction being ⟨100⟩, consistent with the orientation of the starting Si (100) substrates. (c) EDS spectrum of the location "c" of the Si nanopillar tip, again confirming the presence of pure Ag nanoclusters. The signal of Cu comes from the TEM grid while the signals of C and O come from the measuring background.

confirmed with the chemical and structural characterization in electron microscopic studies as indicated in Fig. 3 and 4. It is also noted that these nano-arrays have preserved the crystallinity from the starting substrate, which is in distinct contrast to the template-assisted bottom-up approach.[26]

Anisotropic etching mechanism

More importantly, the Ag nanoclusters were found to be preferentially deposited around the rim of the tip, revealing that the Si atoms in the rim region are more reactive than those in the core region (Fig. 5a). This difference in the reactivity is mainly due to the crystallinity of Si in different regions: the terminal Si atoms in the rim region have lower crystallinity and thus are more reactive towards AgF, in which this rim or edge effect has also been commonly observed in other material systems.[27–29] Upon obtaining the Ag-deposited nanopillars, they were converted to truncated nanopillars by the treatment of HNO_3 to remove the Ag nanoclusters (Fig. 5, step c^1). Nanopencils could then be obtained after multiple Ag nanocluster deposition–removal cycles (Fig. 5, steps b^n and c^n). Therefore, the site-specific reactivity of Si is the key for the anisotropic etching of Si in this work. Moreover, the etching kinetics can be modulated by varying the ratio and the components of the [$AgNO_3$ + HF + HNO_3] mixture to achieve different morphologies. For example, nanocones could be obtained by the addition of extra $AgNO_3$ to HF, in which the extra $AgNO_3$ speeds up the formation of Ag nanoclusters. It is also worth

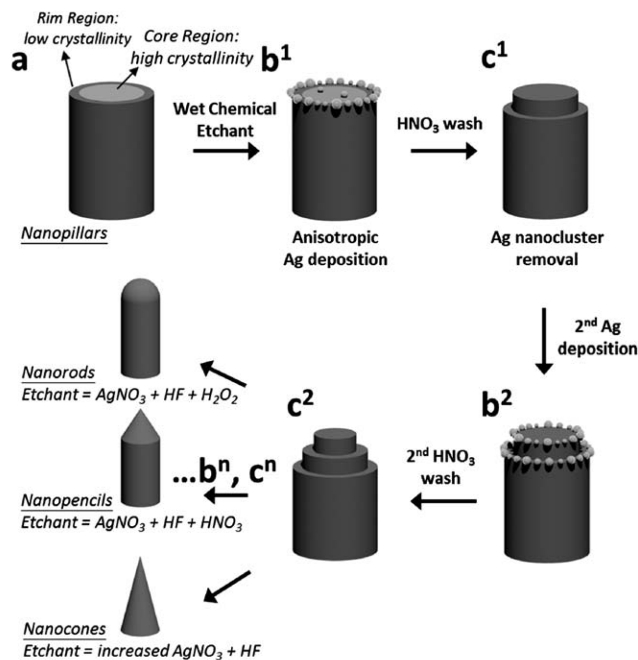

Fig. 5 Schematic illustrations of the formation mechanism of Si nanostructures with different morphologies observed in Fig. 1.

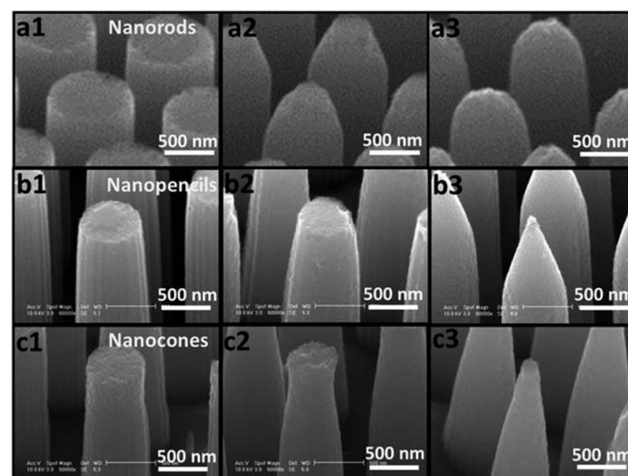

Fig. 6 SEM images depicting the detailed process procedures for the fabrication of (a) nanorod arrays, (b) nanopencil arrays and (c) nanocone arrays (all with the same pitch of 1.3 μm). (a1) Starting nanopillar array template; (a2) after the 1st Ag deposition and acid washing cycle. The etchant is a solution mixture of $AgNO_3$ (0.0002 M), HF (2 M) and H_2O_2 (0.005 M); (a3) after the 3rd Ag deposition and acid washing cycle with the same etchant to obtain the round dome head terminals; (b1) after the 1st Ag deposition and acid washing cycle. The etchant is a solution mixture of $AgNO_3$ (0.0002 M), HF (2 M) and HNO_3 (0.005 M); (b2) after the 2nd and (b3) 5th Ag deposition and acid washing cycles with the same etchant to obtain the pencil head terminals; (c1) after the 1st Ag deposition and acid washing cycle. The etchant is a solution mixture of $AgNO_3$ (0.0004 M) and HF (2 M); (c2) after the 4th and (c3) 7th Ag deposition and acid washing cycles with the same etchant with increasing $AgNO_3$ concentration up to 0.001 M (increment in 0.0001 M) in the final cycle in order to obtain the final shape of nanocones. Notably, distilled water washing is introduced after each process step and all chemical reactions are performed at room temperature.

This journal is © The Royal Society of Chemistry 2013

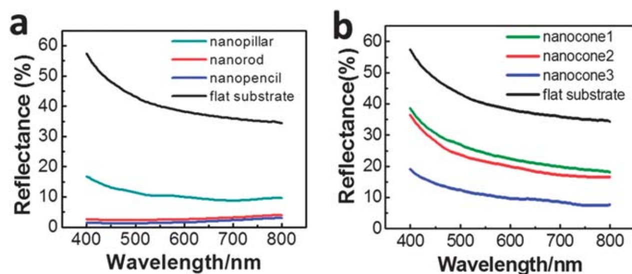

Fig. 7 Optical reflectance measurement of different fabricated morphological nanopillar arrays. (a) Nanopillars, nanorods and nanopencils with the pitch of 0.6 μm. (b) Nanocones with different pitches and aspect ratios (nanocone 1: pitch = 1.3 μm, aspect ratio = 2; nanocone 2: pitch = 0.6 μm, aspect ratio = 2; nanocone 3: pitch = 1.3 μm, aspect ratio = 3).

noting that the use of the [$AgNO_3$ + HF + H_2O_2] system yielded nanorods with the dome head terminal, which may be attributed to the presence of Ag(nanocluster)-catalyzed decomposition of H_2O_2 that modulates the oxidation kinetics of H_2O_2. The detailed process procedures can be found in Fig. 6 for the fabrication of nanorod, nanopencil and nanocone arrays, respectively.

Enhanced photon trapping

In order to investigate the effect of Si nanopillars with different morphological geometries on their light trapping properties, UV-vis reflective spectra were obtained for these structures. Fig. 7a demonstrates the reflectance of 0.6 μm pitch nanopillar, nanorod and nanocone arrays with a 2 μm depth. Particularly, the spectral range of 400–800 nm was chosen to evaluate the optical absorption of these nano-arrays for photovoltaic applications since this wavelength range has covered the peak of solar irradiance.[30] It can be clearly observed that nanorods and nanopencils exhibit drastically reduced reflectance down to <5% as compared to the nanopillar and bare flat substrates, which is mainly due to the tip portion with a smaller pillar diameter for more efficient photon capturing, trapping and transmission down to the base region with a higher material filling ratio and enhanced absorption.[31]

Meanwhile, as presented in Fig. 7b, the reflectance of nanocones (ESI Fig. S2†) is found to reduce significantly for a smaller pitch and higher aspect ratio, agreeing well with the theory for nearly perfect matching between nanocones and air through gradual reduction of the effective refractive index.[32] Notably, further optimization is still in the process in order to assess the performance limits of photon trapping for these nanopencils and nanocones. In any case, all these illustrate the potency of our wet-chemistry-only fabrication approach to achieve the etch anisotropy in various morphological and geometrical nanopillar arrays for large-scale and highly efficient photovoltaics.

Conclusions

In summary, single-crystalline Si nanorod, nanopencil and nanocone arrays have been successfully fabricated with a simple wet-chemistry only fabrication in the large scale. Here, by manipulating the selective deposition of Ag nanoclusters and subsequent etching, the etch anisotropy of these Si nano-arrays can be reliably controlled over large areas, enabling a highly versatile scheme for achieving various Si nanostructures with different morphological geometries for enhanced photon trapping.

Acknowledgements

This research was financially supported by the City University of Hong Kong (Project no. 9667054).

Notes and references

1 M. D. Volder and A. J. Hart, *Angew. Chem., Int. Ed.*, 2013, **52**, 2412.
2 S. Jeong, E. C. Garnett, S. Wang, Z. Yu, S. Fan, M. L. Brongersma, M. D. McGehee and Y. Cui, *Nano Lett.*, 2012, **12**, 2971.
3 Y. Yao, J. Yao, V. K. Narasimhan, Z. Ruan, C. Xie, S. Fan and Y. Cui, *Nat. Commun.*, 2012, **3**, 664.
4 H. Park, S. Choi, J. P. Lee and S. Park, *J. Mater. Chem.*, 2011, **21**, 11996.
5 Y. S. Hu, J. Jeon, T. J. Seok, S. Lee, J. H. Hafner, R. A. Drezek and H. Choo, *ACS Nano*, 2010, **4**, 5721.
6 R. Yu, K. L. Ching, Q. Lin, S. F. Leung, D. Arcrossito and Z. Fan, *ACS Nano*, 2011, **5**, 9291.
7 Y. L. Chueh, Z. Fan, K. Takei, H. Ko, R. Kapadia, N. Miller, K. Yu, M. Wu, E. Haller and A. Javey, *Nano Lett.*, 2010, **10**, 520.
8 X. Fang, Y. Bando, U. K. Gautam, C. Yea and D. Golberg, *J. Mater. Chem.*, 2008, **18**, 509.
9 J. Zhu, Z. Yu, G. F. Burkhard, C. M. Hsu, S. T. Connor, Y. Xu, Q. Wang, M. McGehee, S. Fan and Y. Cui, *Nano Lett.*, 2009, **9**, 279.
10 A. A. Talin, L. L. Hunter, F. Léonard and B. Rokad, *Appl. Phys. Lett.*, 2006, **89**, 153102.
11 J. Goldberger, A. I. Hochbaum, R. Fan and P. Yang, *Nano Lett.*, 2006, **6**, 973.
12 R. Fan, Y. Wu, D. Li, M. Yue, A. Majumdar and P. Yang, *J. Am. Chem. Soc.*, 2003, **125**, 5254.
13 S. W. Schmitt, F. Schechtel, D. Amkreutz, M. Bashouti, S. K. Srivastava, B. Hoffmann, C. Dieker, E. Spiecker, B. Rech and S. H. Christiansen, *Nano Lett.*, 2012, **12**, 4050.
14 K. J. Morton, G. Nieberg, S. Bai and S. Y. Chou, *Nanotechnology*, 2008, **19**, 345301.
15 C. M. Hsu, S. T. Connor, M. X. Tang and Y. Cui, *Appl. Phys. Lett.*, 2008, **93**, 133109.
16 K. L. Klein, A. V. Melechko, J. D. Fowlkes, P. D. Rack, D. K. Hensley, H. M. Meyer, L. F. Allard, T. E. McKnight and M. L. Simpson, *J. Phys. Chem. B*, 2006, **110**, 4766.
17 *Fundamental Aspects of Silicon Oxidation*, ed. Y. J. Chabal, Springer, New York, 2001.
18 K. Peng, M. Zhang, A. Lu, N. B. Wong, R. Zhang and S. T. Lee, *Appl. Phys. Lett.*, 2007, **90**, 163123.
19 K. Peng, A. Lu, R. Zhang and S. T. Lee, *Adv. Funct. Mater.*, 2008, **18**, 3026.

Published on 21 June 2013. Downloaded by City University of Hong Kong on 06/08/2013 11:31:17.

Published on 21 June 2013. Downloaded by City University of Hong Kong on 06/08/2013 11:31:17.

20 H. Robbins and B. Schwartz, *J. Electrochem. Soc.*, 1959, **106**, 505.
21 B. Schwartz and H. Robbins, *J. Electrochem. Soc.*, 1961, **108**, 365.
22 J. K. Kang and C. B. Musgrave, *J. Chem. Phys.*, 2002, **116**, 275.
23 D. M. Knotter, *J. Am. Chem. Soc.*, 2000, **122**, 4345.
24 D. J. Monk, D. S. Soane and R. T. Howe, *Thin Solid Films*, 1993, **232**, 1.
25 R. J. H. Voorhoeve and J. W. Merewether, *J. Electrochem. Soc.*, 1972, **119**, 364.
26 O. Ergen, D. Ruebusch, H. Fang, A. Rathore, R. Kapadia, Z. Fan, K. Takei, A. Jamshidi, M. Wu and A. Javey, *J. Am. Chem. Soc.*, 2010, **132**, 13972.
27 X. H. Yang, F. G. Zeng and X. J. Li, *Mater. Sci. Semicond. Process.*, 2013, **16**, 10.
28 X. H. Yang, W. F. Jiang and X. J. Li, *Thin Solid Films*, 2010, **518**, 6866.
29 Z. Zhang and M. G. Lagally, *Science*, 1997, **276**, 377.
30 S. F. Leung, M. Yu, Q. Lin, K. Kwon, K. L. Ching, L. Gu, K. Yu and Z. Fan, *Nano Lett.*, 2012, **12**, 3682.
31 Z. Fan, R. Kapadia, P. W. Leu, X. Zhang, Y. L. Chueh, K. Takei, K. Yu, A. Jamshidi, A. A. Rathore, D. J. Ruebusch, M. Wu and A. Javey, *Nano Lett.*, 2010, **10**, 3823.
32 Y. F. Huang, S. Chattopadhyay, Y. J. Jen, C. Y. Peng, T. A. Liu, Y. Hsu, C. L. Pan, H. C. Lo, C. H. Hsu, Y. H. Chang, C. S. Lee, K. H. Chen and L. C. Chen, *Nat. Nanotechnol.*, 2007, **2**, 770.

This journal is © The Royal Society of Chemistry 2013